

UNCLASSIFIED

AD NUMBER
AD485854
NEW LIMITATION CHANGE
TO Approved for public release, distribution unlimited
FROM Distribution authorized to U.S. Gov't. agencies and their contractors; Administrative/Operational Use; JUN 1966. Other requests shall be referred to Army Engineer Waterways Station, COE, Vicksburg, MS.
AUTHORITY
USAEWES ltr, 27 Jul 1971

THIS PAGE IS UNCLASSIFIED

TECHNICAL REPORT NO. 3-729

# MECHANICS OF WHEELS ON SOFT SOILS A METHOD OF ANALYZING TEST RESULTS

by

E. M. Leflaive



June 1966

Sponsored by

U. S. Army Materiel Command  
Task No. 1-V-0-14501-B-52A-01

Best Available Copy

Conducted by

U. S. Army Engineer Waterways Experiment Station  
CORPS OF ENGINEERS  
Vicksburg, Mississippi

ARMY-MRC VICKSBURG, MISS.

This document is subject to special export controls and each transmittal to foreign governments or foreign nationals may be made only with prior approval of U. S. Army Engineer Waterways Experiment Station.

AD-485 854

## FOREWORD

The study reported herein was performed by Dr. E. M. Leflaive at the U. S. Army Engineer Waterways Experiment Station (WES) utilizing funds and resources furnished by the Directorate of Research and Development, U. S. Army Materiel Command, under DA Task 1-V-O-14501-B-52A-01, "Earth Physics, (Terrain Analysis)."

The U. S. Army Research Office-Durham (ARO-D) negotiated contract No. DA-31-124-ARO(D)-164 with Duke University for the employment of Dr. Leflaive for one year. With the cooperation of ARO-D and at the request of Mr. W. J. Turnbull, Technical Assistant for Soils and Environmental Engineering, WES, Dr. Leflaive was assigned to WES in October 1963 for the duration of his contract. At the expiration of the contract, Dr. Leflaive became a member of the staff of the Mobility Section, Army Mobility Research Branch (AMRB), Mobility and Environmental Division, WES.

Technical assistance and the test data that were employed in the study were provided by personnel of the AMRB. This report was prepared by Dr. Leflaive.

Col. Alex G. Sutton, Jr., CE, and Col. John R. Oswalt, Jr., CE, were Directors of the WES during the study and the preparation of this report. Mr. J. B. Tiffany was Technical Director.

## CONTENTS

	<u>Page</u>
FOREWORD . . . . .	iii
SUMMARY . . . . .	vii
PART I: INTRODUCTION . . . . .	1
Background . . . . .	1
Purpose and Scope . . . . .	1
Definitions and Notation . . . . .	2
PART II: DEVELOPMENT OF THE ANALYSIS METHOD . . . . .	5
Energy Concept . . . . .	5
Exposition of the Reference System . . . . .	6
PART III: ANALYSIS OF TEST RESULTS . . . . .	9
Data Examined . . . . .	9
Parameters Considered . . . . .	10
Deviations of Experimental Results from Reference System . . . . .	10
Comparisons Among Various Tires . . . . .	16
PART IV: CONCLUSIONS AND RECOMMENDATIONS . . . . .	19
Conclusions . . . . .	19
Recommendations . . . . .	20
PLATES 1-3	
APPENDIX A: COMPARISON OF NORMAL SLIP AND DIFFERENTIAL SLIP . . . . .	A1
Definitions . . . . .	A1
Values of Normal and Differential Slip Under Various Operating Conditions of the Wheel . . . . .	A1
Properties of Normal and Differential Slip . . . . .	A2
APPENDIX B: INFLUENCE OF STRESS DISTRIBUTION ON TORQUE . . . . .	B1
APPENDIX C: ROTATIONAL DIRECT SHEAR TESTS ON YUMA SAND . . . . .	C1
APPENDIX D: CRITERIA FOR PROPELLING-SYSTEM EFFICIENCY . . . . .	D1
Size and Efficiency . . . . .	D1
Means of Expressing Efficiency . . . . .	D2
Combination of Efficiency Coefficients and Indexes . . . . .	D6

## SUMMARY

This report presents a method of analyzing the results of tests with pneumatic tires in sand. The method is based on considering the work of the pull developed by the test wheel as the difference between energy input and energy dissipation. The parameters used to represent these energies are defined, and their meanings are described in some detail by referring to the theoretical case of a rigid wheel on a rigid surface. This theoretical case is also used as a reference system to evaluate the results of actual tests. Experimental data for a number of representative test conditions are presented and compared with the reference system. Concepts of efficiency are introduced and discussed.

It is concluded that the proposed approach is promising for both conveniently expressing experimental results and understanding tire behavior in soft soils. However, more data will have to be analyzed to draw quantitative conclusions for practical use.

Four appendixes are included in which certain aspects of the definitions of slip, stress distribution, lateral confinement of sand, and criteria for propelling-system efficiency are discussed.

MECHANICS OF WHEELS ON SOFT SOILS;  
A METHOD OF ANALYZING TEST RESULTS

PART I: INTRODUCTION

Background

1. In 1960, under the sponsorship of the U. S. Army Materiel Command, a research program was initiated at the U. S. Army Engineer Waterways Experiment Station (WES) to study the performance of soils under tire loads. Many tests have been run with several pneumatic tires in soft soils during this program. The tests were conducted in specially prepared soil bins with a single-wheel dynamometer carriage that was capable of measuring pertinent moments, forces, and displacements of the test system. The test program, equipment, and facilities, as well as the specific test results, are described in a series of reports under the general title Performance of Soils Under Tire Loads.\*

2. The study reported herein was begun as a result of recognition of the need for a better understanding of the interaction of soils and pneumatic tires. Some tire-soil relations observed in the test results could not be adequately described on the basis of the present understanding of the mathematics of such systems. Additional stimulus was gained from a paper\*\* presented at the First International Conference on Soil-Vehicle Systems in which a concept of rolling resistance was discussed in detail.

Purpose and Scope

3. While this report is concerned with the task of furthering our understanding of the mechanics of wheels operating on soft soils, it is

---

\* U. S. Army Engineer Waterways Experiment Station, CE, Performance of Soils Under Tire Loads, Technical Report No. 3-666, Reports 1-5, Vicksburg, Miss.

\*\* J. R. Phillips, "The powered vehicular wheel plane-rolling in equilibrium: a consideration of slip and rolling resistance," Mechanics of Soil-Vehicle Systems: First International Conference on Mechanics of Soil-Vehicle Systems (Turin, Italy, June 1961), pp 541-544.

principally an attempt to develop and demonstrate a useful method of analyzing experimental results.

4. The program of performance of soil's under tire loads was essentially of exploratory nature. Interpretation of such tests required a general view of the meaning of the test results. Difficulty stemmed from the numerous parameters and variables that play a part in rolling motion. Thus, the problem was to decide in what terms test results should be expressed and plotted to obtain a convenient and instructive description of experimental facts. It is with this problem that this report is concerned.

5. Data from 44 tests conducted on air-dry sand (Yuma sand) were used both to develop and evaluate the method of analysis. General qualitative conclusions are offered, but no attempt is made to draw definite quantitative conclusions for practical use.

6. The importance of considering efficiency for wheel performance evaluation is emphasized in this report. Efficiency evaluation is considered an element of test interpretation because of its usefulness in comparing the performance of different wheels.

#### Definitions and Notation

7. Definitions of terms peculiar to this report are given below. Other pertinent definitions can be found in WES Technical Report No. 3-666, Report 1. Notation for pertinent quantities used in the definitions is as follows:

M = torque	v = translation speed
P = pull	R = radius of the wheel
$\omega$ = rotational velocity of the wheel (radians/sec)	W = vertical load
	t = time

#### Slip terms

8. Two definitions of slip are used and are referred to as normal slip  $s$  and differential slip  $g$ . They are defined as:

$$s = \frac{\text{theoretical velocity} - \text{actual velocity}}{\text{theoretical velocity}}$$

$$g = \frac{\text{theoretical velocity} - \text{actual velocity}}{\text{actual velocity}}$$

The word "normal" means the constant value taken as a reference in the denominator. The word "differential" stresses the variable character of the actual distance taken as a reference. These adjectives are used whenever the distinction is necessary. The term "slip" used alone means the physical phenomenon of slip, whenever its numeric value is unimportant.

9. Normal slip and differential slip are, respectively,

$$s = \frac{R_0 - v}{R_0} = 1 - \frac{v}{R_0}$$

$$g = \frac{R_0 - v}{v} = \frac{R_0}{v} - 1$$

Therefore,

$$g = \frac{s}{1 - s}$$

and

$$s = \frac{g}{1 + g}$$

A comparison of normal slip and differential slip is given in detail in Appendix A.

#### Energy terms

10. Three dimensionless energy coefficients are defined as follows.

- a. Torque energy coefficient  $\eta$  is the energy supplied or withdrawn at the wheel axle, per unit of vertical load, per unit of distance traveled by the wheel. Thus,

$$\eta = \frac{M_0}{Wv} = \frac{M}{WR} \frac{1}{1 - s} = \frac{M}{WR} (1 + g)$$

- b. Pull energy coefficient  $\lambda$  is the energy recovered or supplied as a pull, per unit of load, per unit of distance traveled. Algebraically,

$$\lambda = \frac{Pv}{Wv} = \frac{P}{W}$$

Thus, it is seen that the pull energy coefficient  $\lambda$  is also the ratio  $\frac{\text{pull}}{\text{load}}$ .

- c. Dissipated energy coefficient  $\rho$  is the energy not recovered



mechanically, per unit of load, per unit of distance traveled.  
Therefore,

$$\rho = \eta - \lambda = \frac{M_D}{W_V} - \frac{P}{W}$$

The dissipated energy coefficient  $\rho$  is identical with the coefficient of rolling resistance proposed by Phillips.\*

#### Efficiency

11. The efficiency parameter used in the analysis is termed the "traction efficiency." (Other definitions of efficiency are given in Appendix D.) The traction efficiency  $\tau$  is

$$\tau = \frac{\lambda}{\eta - \eta_a}$$

where  $\eta_a$  is the torque energy expended when the wheel is just barely propelling itself. The traction efficiency  $\tau$  is the ratio of the energy available as pull energy to the increment of torque energy (in excess of the torque energy required for self-propulsion) that must be expended to produce the pull.

---

\* See footnote on page 1.

## PART II: DEVELOPMENT OF THE ANALYSIS METHOD

### Energy Concept

#### Primary considerations

12. The method of analysis developed in this report is based on equating the energy supplied or withdrawn at the wheel axle (torque energy), the energy made available as pull (pull energy), and the energy dissipated in the soil and in the tire. From the test data, the torque energy and the pull energy can be determined. The dissipated energy is the difference between the torque energy and the pull energy and therefore is also known. The variations of the torque energy and of the dissipated energy are studied as functions of the test conditions. If relations can be shown between the test conditions and these two energies, these can be predicted. Then the pull can be predicted also.

13. The purpose in selecting this approach is to provide a relatively simple method of describing the wheel-soil interaction and to separate the principal phenomena that determine the test results. From the physical viewpoint, it is useful to consider the process involving the energy input to be independent of the process by which energy is lost to the soil. Evidently the two processes are related because both are affected by the basic test parameters and by the secondary phenomena that occur while a wheel is in motion, such as effect of sinkage on boundary conditions, change in soil density due to shear, etc. However, it is proposed to consider the two phenomena separately and to regard the pull as the result of their superposition.

14. Another reason for considering energies is their suitability for dealing with efficiency. The problem of the efficiency of a wheel is discussed in Appendix D. Various efficiency coefficients are defined that are ratios of energy quantities based on torque, pull, and dissipated energies used for analyzing test results.

#### Reference condition

15. The energy concept is made meaningful by comparing the energies associated with a pneumatic tire operating in soil with the corresponding

### Exposition of the Reference System

**LEGEND**

SYMBOL	COEFFICIENT
M	TORQUE
P	PULL ENERGY
f	DISSIPATED ENERGY
f	TORQUE ENERGY
f	FRICTION

$\omega$  AND V  
IN OPPOSITION

BRAKING WHEEL

DRIVING WHEEL

NONROTATING WHEEL

energy, and dissipated energy coefficients are plotted versus differential slip  $g$ . The plots are described in the following paragraphs.

17. The torque  $M$  is limited by the maximum frictional force at

the contact point. It has the value  $+f$  for any positive differential slip and  $-f$  for any negative differential slip. For zero slip,  $M$  can have any value between  $+f$  and  $-f$ . Since both  $W$  and  $R = 1$ , the torque energy coefficient  $\eta$  is equal to  $M(1 + g)$  (see paragraph 10). Thus, for  $g > 0$ ,

$$\eta = +f(1 + g)$$

for  $g = 0$ ,

$$\eta = M$$

and for  $g < 0$ ,

$$\eta = -f(1 + g)$$

The point  $g = -1$  corresponds to a nonrotating wheel (normal slip infinite); between  $g = 0$  and  $g = -1$ , the wheel is braked and energy is withdrawn from the wheel; and for  $g < -1$ , positive energy is supplied to rotate the wheel in a direction opposing its movement.

#### Dissipated energy coefficient $\rho$

18. The dissipated energy coefficient  $\rho$  is the energy absorbed by friction between the wheel and the surface. For zero slip, there is no friction, so  $\rho = 0$ . For a given slip, energy absorbed by friction for one unit of distance traveled by the wheel is equal to the product of the frictional force and the relative displacement of the wheel and soil surfaces during the corresponding time. The friction force is  $\pm f$  ( $-f$  for  $g < 0$ ); the soil-wheel displacement when the wheel travels one unit of distance is  $g$  (from the definition of differential slip). Therefore,  $\rho = \pm fg$  ( $-f$  for  $g < 0$ ), as shown in fig. 1.

#### Pull energy coefficient $\lambda$

19. The pull energy coefficient  $\lambda$  is equal to the torque energy coefficient  $\eta$  when slip is zero. For positive differential slip,  $\lambda = +f$ ; for negative differential slip,  $\lambda = -f$ . Considering the changes of  $\eta$ ,  $\rho$ , and  $\lambda$  as slip increases, the increase in torque energy is exactly absorbed by the corresponding increase in dissipated energy and thus pull remains constant. This result may appear obvious for the theoretical reference condition; however, it is mentioned because for a

wheel rolling on a real soil, the torque energy and the dissipated energy do not usually vary in such a parallel manner.

Traction efficiency  $\tau$

20. Fig. 2 represents the variation of traction efficiency  $\tau$  with

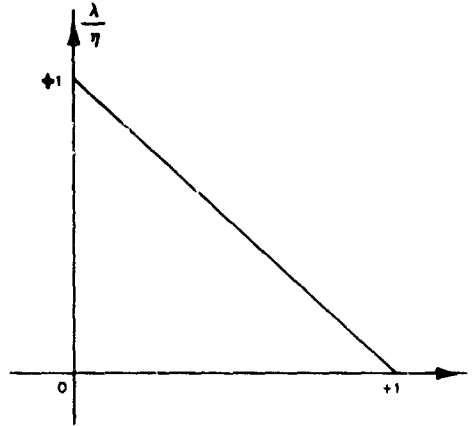


Fig. 2. Traction efficiency  $\tau$  (or  $\frac{\lambda}{\eta}$ ) for a rigid wheel on a rigid ground

respect to normal slip  $s$ . Since the torque energy coefficient for self-propulsion  $\eta_a$  is zero for the theoretical reference condition,

$$\tau = \frac{\lambda}{\eta - \eta_a} = \frac{\lambda}{\eta} = \frac{\eta - \rho}{\eta} = \frac{\pm f(1 + g) - (\pm f g)}{\pm f(1 + g)} = \frac{1}{1 + g} = 1 - s$$

### PART III: ANALYSIS OF TEST RESULTS

#### Data Examined

21. Test data were examined to evaluate the application of the proposed method of analysis. The data were obtained from programmed-slip tests performed with smooth pneumatic tires in air-dry Yuma sand.

22. One tire, the 9.00-14, 2-PR, buffed smooth, was studied in a fairly thorough manner. Results of 18 tests with this tire, representing a wide range of load, deflection, and cone index conditions, were examined. The effects of load, deflection, and cone index on test results were studied by the proposed method of analysis. Another group of test data obtained with tires of very different shapes was used to explore the influence of the tire dimensions. Six tests were with the bicycle tire (1.75-26), five with the Terra-Tire (16-15-6R, 2-PR), and two with the 4.50-7, 2-PR tire. All tires were buffed smooth. The results show the extent to which the method is valid for different tire shapes, and how the performance curves are affected by the shape. A third group of data, obtained from 13 tests with the 4.50-18, 4-PR smooth tire, was analyzed, but because of unexplainable inconsistencies in the data, these tests have not been included in the analysis.

23. The test conditions from which data were obtained for analysis are listed below.

<u>Tire Size</u>	<u>Deflection %</u>	<u>Load lb</u>	<u>Approximate Test Cone Index</u>
9.00-14, 2-PR	15	455	25, 45, 65
		670	25, 45, 65
		890	25, 45, 65
	35	455	25, 45, 65
		720	25, 45, 65
		1225	25, 45, 65
4.50-18, 4-PR	15	455	25, 45, 65
		890	25, 45, 65
	35	455	25, 45, 65
		890	25, 45, 65
		1440	53

(Continued)

<u>Tire Size</u>	<u>Deflection %</u>	<u>Load lb</u>	<u>Approximate Test Cone Index</u>
4.50-7, 2-PR	35	225	55
		455	55
1.75-26	15	100	25, 65
		225	25, 65
	35	100	25
		225	25
16-15-6R, 2-PR	25	225	20, 55
		455	20, 55
		720	55

#### Parameters Considered

24. In Part II, the four quantities defined as the basic parameters involved in the method of analysis were torque energy coefficient  $\eta$ , pull energy coefficient  $\lambda$ , dissipated energy coefficient  $\rho$ , and traction efficiency  $\tau$ . Only two of these, torque energy and dissipated energy coefficients, are considered in the present test analysis. The pull energy coefficient is not studied directly because it is a principle of the method to regard it as the algebraic sum of torque energy and dissipated energy. Traction efficiency  $\tau$  has not been studied in enough detail to be reported.

#### Deviations of Experimental Results from Reference System

25. Wheels rolling in soils do not behave in the ideal manner shown in the reference system in fig. 1. This is both a predictable result and an experimental fact. In the following paragraphs, predictable differences are discussed first, and then ideal and actual conditions are compared on the basis of the test data. Comparison of fig. 1 with test results shown in figs. 3 and 4 shows that there is still enough similarity between actual and ideal behavior to expect a meaningful comparison.

#### Comparisons based on predictable differences be- tween actual and ideal conditions

26. The main reasons to expect differences between actual and ideal

Fig. 3. Torque energy coefficient as a function of differential slip (an example of experimental result)

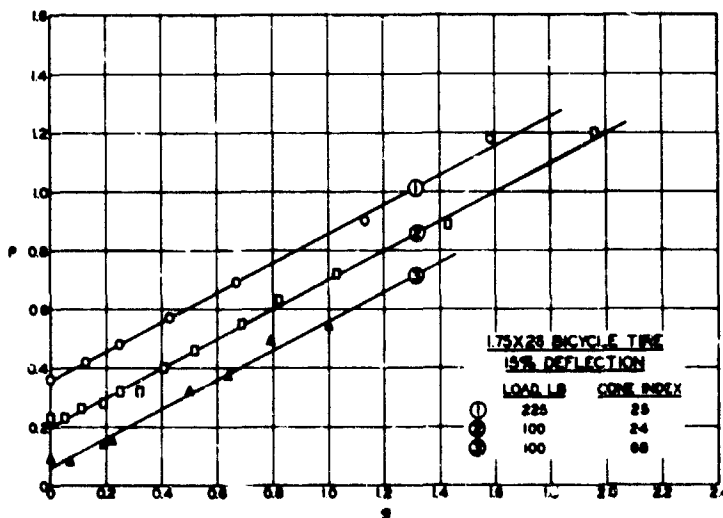
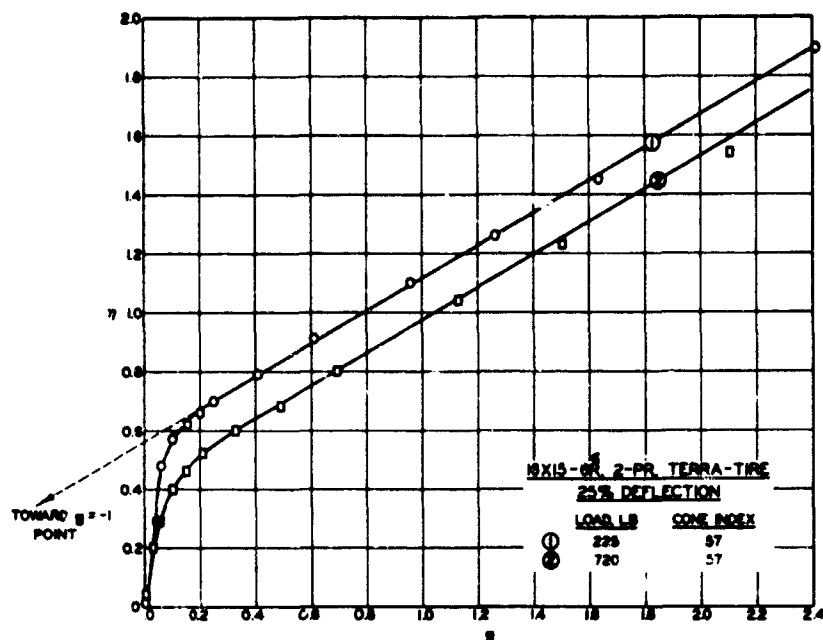
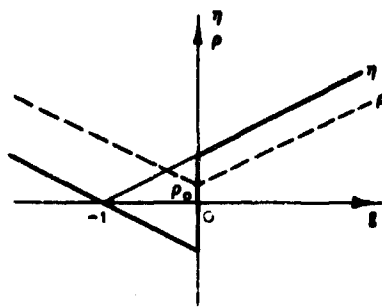


Fig. 4. Dissipated energy coefficient as a function of differential slip (an example of experimental result)

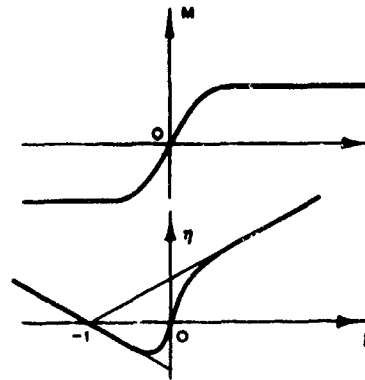
conditions are (a) the wheel sinks in the soil, (b) the soil must be deformed in the direction of the wheel movement to develop frictional resistance in this direction, and (c) actual conditions are three-dimensional.

27. Since the wheel sinks at zero slip, the dissipated energy coefficient  $\rho$  is not zero at zero slip under actual conditions, but has a certain value  $\rho_0$ . Therefore, the dissipated energy curve can be expected to

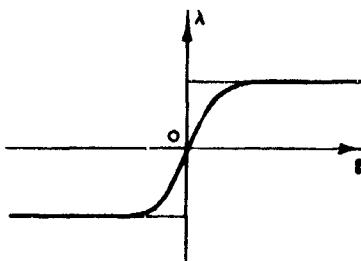




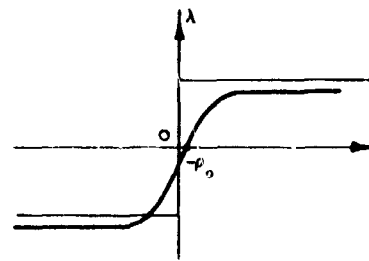
a. System for energy coefficient, considering energy loss due to sinkage at zero slip



b. System for torque and torque energy coefficient, considering progressive increase of torque with slip



c. System for pull energy coefficient, considering progressive increase of torque with slip



d. System for pull energy coefficient, considering both energy loss due to sinkage at zero slip and progressive increase of torque with slip

Fig. 5. Modified reference system diagrams

resemble that shown in fig. 5a. Sinkage also results in a certain length of contact between the wheel and the soil, and the torque may be affected through the resulting stress distribution.

28. The relative soil-wheel displacement in the direction of the wheel movement needed to develop friction in its direction for the actual wheel leads to a torque versus slip curve with a finite slope near the origin. This finite slope and the approximate torque energy coefficient curve that results are shown in fig. 5b. The pull energy coefficient curve that would result, with the original dissipated energy  $\rho$  versus slip  $g$

( $\rho_0 = 0$ ) curve, is shown in fig. 5c. The pull energy coefficient  $\lambda$  curve resulting when both sinkage and soil yielding under shear are considered is shown in fig. 5d. It was obtained by translating downward the curve in fig. 5c and shows that slip at the point of self-propulsion ( $\lambda = 0$ ) is a function of both  $\rho_0$  and the shape of the torque versus slip curve.

29. The third main difference between wheels and the reference condition involves the effect of stresses and deformations normal to the plane of the wheel. The three-dimensional pattern of the flow of the soil under the moving wheel is believed to be a fundamental characteristic of its behavior. However, discussion of this effect is too complex to be developed at the present time. (One aspect of the problem is considered in Appendix C.)

Comparison based on  
observed differences be-  
tween actual and ideal conditions

30. Torque and torque energy. Plate 1 shows torque energy coefficient  $\eta$  plotted versus differential slip  $g$ . Usually, the torque is not zero at zero slip. As load increases or cone index decreases, larger positive values of torque  $M$  and torque energy coefficient  $\eta$  are obtained at zero slip. However, in most conditions, the values of torque energy coefficient at zero slip are small compared with the values of dissipated energy coefficient  $\rho$  at the same slip.

31. Another observation concerns the slopes of the torque energy coefficient curves in the small slip range for various cone index conditions. It is logical that the lower the cone index is, the smaller is the slope because a looser sand needs a larger deformation to develop shear strength. This is best seen on the Terra-Tire data (plate 1).

32. The torque energy coefficient curves change slope when differential slip reaches values between 20 and 40 percent. At this point, the friction of the soil probably is fully mobilized; however, torque and torque energy coefficients do not have the same values at this point for different test conditions. A very consistent result is that torque energy coefficient at a given slip is smaller when the cone index is low or when the load is high, or both. Thus, for constant slip and tire radius, the

torque/load ratio is smaller for larger loads or for lower cone indexes. This decrease of torque energy is important quantitatively. The amount of decrease for the range of conditions under study is as great as 0.20. Since the pull energy coefficient  $\lambda$  which is equal to torque energy coefficient minus dissipated energy coefficient ( $\eta - \rho$ ) seldom exceeds 0.50 in the sand, this decrease in torque energy of 0.20 is of primary importance. So far, no theory has predicted a decrease in torque/load ratio associated with a load increase. A possible explanation may be found in the combined effects of load, wheel geometry, and slip on the three-dimensional pattern of the flow of the sand, combined with the relation between torque and stress distribution (see Appendix B).

33. Generally, for a particular tire size, the test curve conformed most closely to the ideal condition curve at the lowest loads and greatest soil densities. Tests with very low loads on relatively large tires and with high cone indexes showed torque energy coefficient  $\eta$  versus slip  $g$  curves virtually identical with a theoretical straight line intersecting the  $g$  axis at  $g = -1$ , as suggested by fig. 1 (also see curve in upper right plot of plate 1 for 455-lb load, 65 cone index). This line is an upper boundary in the  $\eta$  versus  $g$  graph. The curves below this line are approximately parallel for each tire. Therefore the slope of these lines appears to be characteristic of the performance of each particular wheel, and indicates the maximum torque/load ratio that can be attained with that wheel.

34. In the reference system, the slope of the torque energy coefficient versus differential slip line is equal to the coefficient of friction between the wheel and the surface on which it rolls. Experimental data yielded torque energy curves (plate 1) with definite slopes, and it would be of interest to compare these slopes with the tangent of the angle of friction of the sand. However, the way to measure the angle of friction to give a meaningful comparison presents a problem. Torque energy coefficient lines are straight for slips larger than 20 and 30 percent. For such slips, the sand is subjected to large strains, in terms of soil mechanics; therefore, the angle of friction should be determined for correspondingly large deformations. Because such measurements are not readily available,

the comparison could not be made. See Appendix C for information on shear tests on Yuma sand.

35. Dissipated energy. The dissipated energy coefficient versus differential slip curves are approximately straight (see plate 2). For a given tire at a given deflection, the slopes of the dissipated energy coefficient lines for various load and cone index conditions were the same. These slopes were not affected by  $\rho_0$ , the dissipated energy coefficient at zero slip. Therefore, the dissipated energy coefficient can be expressed as

$$\rho = \rho_0 + \rho'$$

For a given wheel,  $\rho_0$  depends upon load and cone index and represents the work necessary for the wheel to penetrate the sand while it is rolling at zero slip. This penetration is primarily required to develop the bearing capacity of the soil. The work absorbed by slip is represented by  $\rho'$ . It arises from the mechanical process in which slip friction is developed and the slipping wheel digs the rut by carrying the sand rearward. This process is not primarily related to bearing capacity, but as theoretically expected produces a resisting work proportional to differential slip.

36. For an understanding of wheel behavior in soft sand, it is of major importance to note that generally the slope of the dissipated energy coefficient curves for a given wheel is different from the final slope of the torque energy coefficient curves for the same wheel. Since the pull energy coefficient is equal to the torque energy coefficient minus the dissipated energy coefficient ( $\lambda = \eta - \rho$ ), this difference results in an increase or decrease of the pull energy coefficient with slip in the large slip range (plate 3). In fact, this difference was consistently found to be a decrease, except for the bicycle tire for which there was no variation. The difference in slope of the torque energy coefficient  $\eta$  and dissipated energy coefficient  $\rho$  curves was therefore responsible for the existence of a maximum pull. The great difference apparent between theoretical and actual conditions in this respect justifies the concept of considering torque input and energy dissipation to be two distinct phenomena and pull to be the result of their interaction. Thus far, no theory has predicted

this difference in variation of input and dissipation with respect to slip. A possible explanation eventually may be found in the effect of slip on the three-dimensional pattern of the flow of the sand as influenced by the wheel geometry, combined with the relations existing between flow pattern and stress distribution on one hand, and flow pattern and energy dissipation on the other.

### Comparisons Among Various Tires

37. The limited number of test results studied so far, with respect to the number of parameters involved in a pneumatic tire rolling on soft soil, does not permit definite conclusions connecting a specific parameter to a specific effect. The purpose of this section is rather to illustrate the usefulness of the proposed approach by indicating ways of interpreting the influence of tire characteristics on torque energy and dissipated energy diagrams.

#### Change in slope on torque energy diagrams

38. From the zero slip range, the torque energy coefficient first increases at a rate that depends upon the cone index of the soil. Next it reaches a transition zone where the slope of the curve flattens, and then it varies along a straight line (constant rate of increase). The point T at which the straight line begins is reached at a certain differential slip  $g_1$ . Experimental curves showed that slip  $g_1$  is approximately the same for a given tire regardless of load and cone index conditions, but may be different for different tires. These experimentally derived slip values are:

<u>Tire</u>	<u>Differential Slip <math>g_1</math> , %</u>	<u>Normal Slip <math>s_1</math> , %</u>
1.75-26 (bicycle tire)	50	33
4.50-18	30	23
9.00-14	30	23
16-15-6R (Terra-Tire)	20	17

This suggests that the wider the tire, the sooner the point T is reached. As a whole, this is a reasonable conclusion, if considered only in terms of

confinement of soil under shear according to the shape of the contact area. However, a correct interpretation must consider many other factors besides width/diameter ratio. This property of reaching high torque energy at low slips is of practical interest as far as efficiency is concerned, because the dissipated energy coefficient increases linearly with slip.

Slope of torque energy  
coefficient curves at large slips

39. The slope of the straight portions of the torque energy coefficient curve is denoted by  $\tan \alpha$ . Values of  $\tan \alpha$  between 0.51 and 0.58 usually were obtained in the test results, but values outside this range were noted, especially for the 4.50-18 tire and for one test with the bicycle tire. Values of  $\tan \alpha$  that are believed reliable are 0.51 or 0.52 for the 9.00-14, 2-PR tire and the bicycle tire and 0.56 for the Terra-Tire. The data for the 4.50-18 tire were not sufficiently consistent to designate a value of  $\tan \alpha$  for this tire. Since the values for the other tires are close together, it was concluded that tire characteristics do not significantly affect the ability of the tire to develop a certain torque ratio,\* provided a sufficiently large slip is attained. However, the shape of the Terra-Tire did favor slightly larger torque ratios.

Slope of dissipated  
energy coefficient lines

40. The slope of the dissipated energy coefficient lines is denoted by  $\tan \beta$ . From the test data appreciable differences in the values of  $\tan \beta$  were found for the different tires.

<u>Tire</u>	<u><math>\tan \beta</math></u>	<u><math>\beta</math>, deg</u>
1.75-25 (bicycle tire)	0.50	27
9.00-14	0.60	31
16-15-6R (Terra-Tire)	0.72	36

$\tan \beta$  for the 4.50-18 tire was not considered because of discrepancies

---

\* The torque ratio at a given point of the torque energy curve is the slope of the straight line drawn from the  $g = -1$  point on the  $g$  axis to the point under consideration on the torque energy curve. Thus, the ratio is:  $\frac{\eta}{1+g} = \frac{M}{WR} \frac{(1+g)}{(1+g)} = \frac{M}{WR}$ .

found in the diagrams and because more recent data (not reported herein) give different indications.

41. Although other factors may be involved, the values of  $\tan \beta$  showed very clearly the influence of tire proportions. The importance of this influence can be shown by comparing a test of the bicycle tire with one of the Terra-Tire. In making this comparison, it has been assumed that both have the same torque energy coefficient curve and conditions are such that dissipated energy coefficient  $\rho_0$  at zero slip is negligible. As already stated, pull energy coefficient  $\lambda$  is equal to  $\eta - \rho$ . Therefore, the variation from 0.50 to 0.72 for  $\tan \beta$  means that if the pull energy coefficient at 50 percent normal slip ( $g = 1$ ) were 0.4 for the bicycle tire, it would be only 0.18 for the Terra-Tire at the same slip. Thus, from the standpoint of pull, the rate of increase of dissipated energy coefficient with slip is important. The rate of increase of dissipated energy coefficient  $\rho$  is also important in determining efficiency, since for the powered wheel  $\rho$  is the difference between input and output. Because the value of  $\tan \beta$  is appreciably different for different tires, it is concluded that this factor represents a very significant characteristic of tire behavior in sand.

#### PART IV: CONCLUSIONS AND RECOMMENDATIONS

##### Conclusions

42. The case of a powered rigid wheel rolling on an incompressible surface was examined to determine its utility as a datum, or reference, upon which to base an analysis of pneumatic-tired wheels rolling in yielding sand. The examination revealed considerable merit in this method of analysis. The following advantages were shown:

- a. The reference condition provided straightforward means of separate consideration of the energy input coefficient  $\eta$  and the energy dissipation coefficient  $\rho$ . The pull coefficient  $\lambda$  is regarded as the difference between  $\eta$  and  $\rho$ .
- b. Comparison of actual data (on the pneumatic-tired wheel) with similar information provided by the reference condition was feasible and appeared to be useful.
- c. Relations that varied linearly under the reference condition ( $\eta$  versus  $g$  and  $\rho$  versus  $g$ ) also varied linearly using actual data, at least for a significant portion of the range of data covered (plates 1 and 2).
- d. The slopes  $\eta/g$  and  $\rho/g$ , identical in the reference condition, were found to be different for actual data. This fact appears to justify a need for separate study of the two energy quantities  $\eta$  and  $\rho$ .
- e. The resulting  $\lambda$  versus  $g$  curve ( $\lambda = \eta - \rho$ ) for actual data was not the straight line with zero slope that results from the reference condition.
- f. Differences between actual data and reference data were considered to be attributable to the sinkage necessary for bearing capacity, the slip necessary for mobilizing shear strength in the direction of movement, and three-dimensional deformation and stresses.

43. Data studies at present do not permit complete numerical presentation. However, they warrant the conclusion that the method of



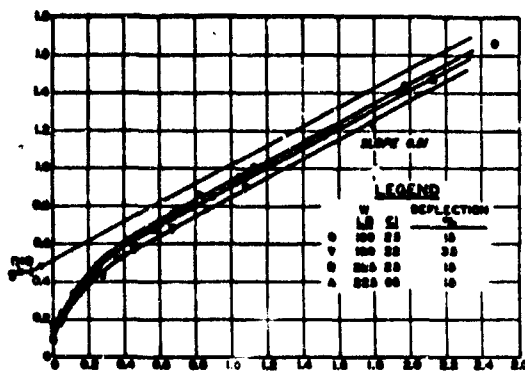
analysis yields means of characterizing quantitatively the general behavior of a tire by use of the parameters of the energy coefficient curves which remain constant when load and sand strength vary.

#### Recommendations

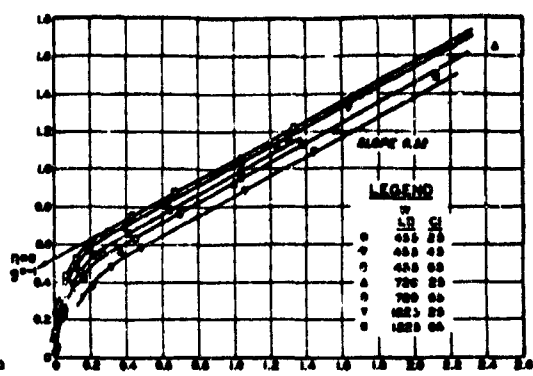
44. The following recommendations are made:

- a. Tests should be performed with rigid wheels of two diameters and three different width/diameter ratios. Such tests would permit an evaluation of the influence of wheel dimension and width on the performance of wheels, as represented by the shape of the torque energy coefficient curves and the slope of the dissipated energy coefficient curves. The use of rigid wheels with rectangular cross section would eliminate the influence of tire deformability and the influence of shape of tire cross section.
- b. Tests should be performed with rigid wheels of different cross-section shapes to study the influence of this factor on wheel performance, as represented by torque energy and dissipated energy coefficient curves.

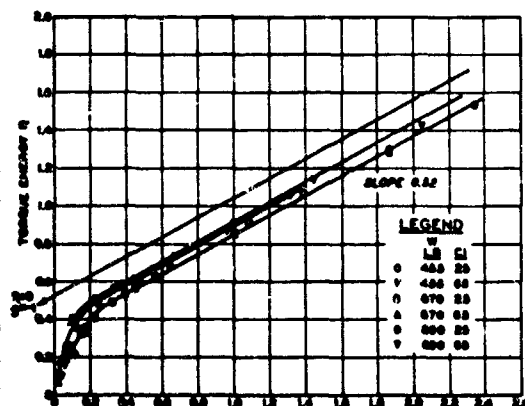
The recommended tests would contribute to the understanding of the differences observed in performances of pneumatic tires.



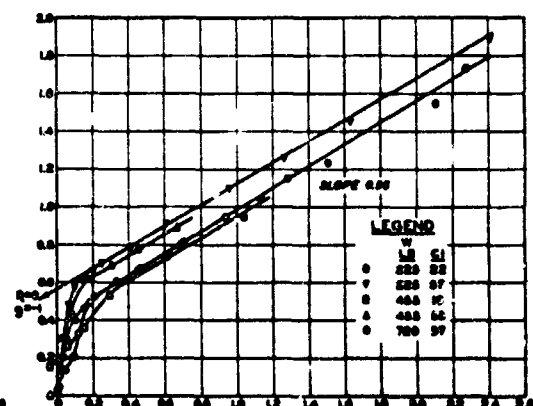
**BICYCLE TIRE**



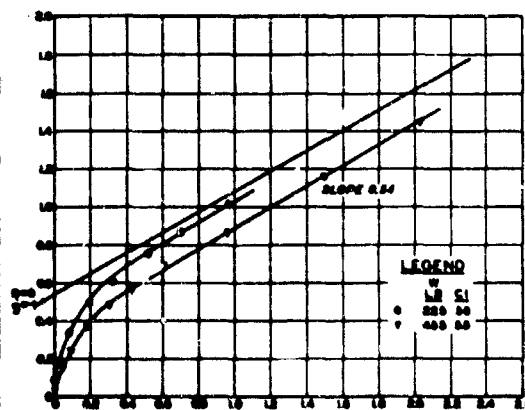
**900-14, 2-PR TIRE  
35% DEFLECTION**



**900-14, 2-PR TIRE  
18% DEFLECTION**

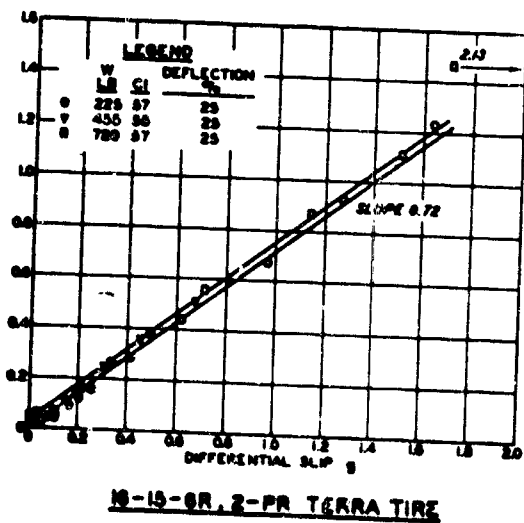
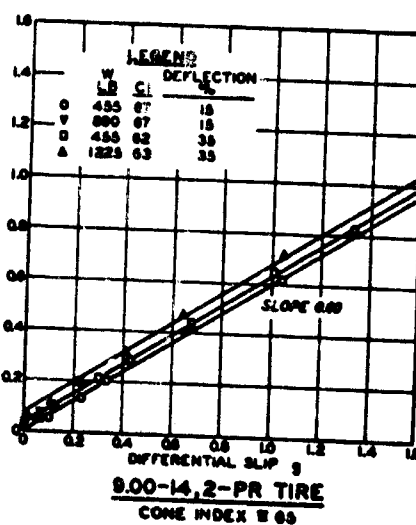
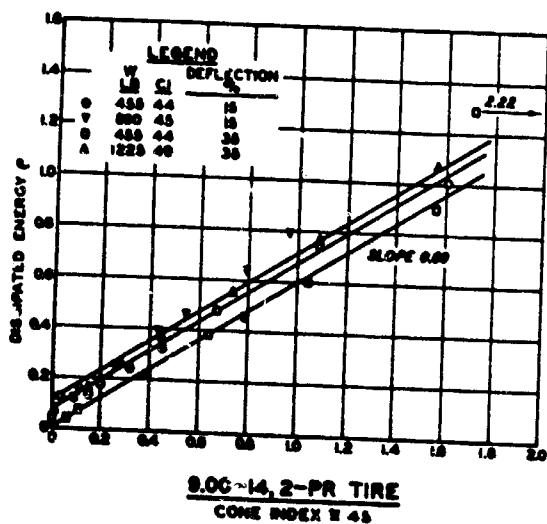
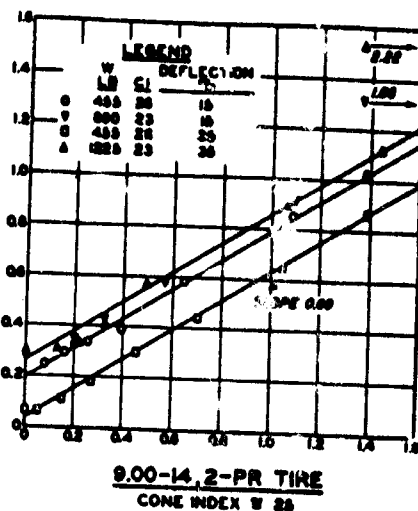
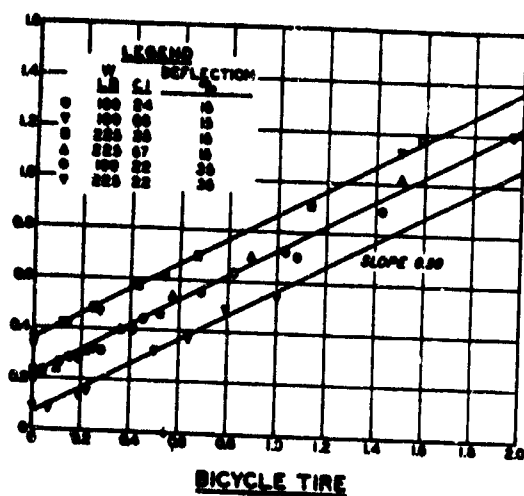


**18-15-6R, 2-PR TERRA TIRE  
25% DEFLECTION**



**450-7, 2-PR TIRE  
30% DEFLECTION**

**TORQUE ENERGY VS  
DIFFERENTIAL SLIP**



## DISSIPATED ENERGY VS DIFFERENTIAL SLIP

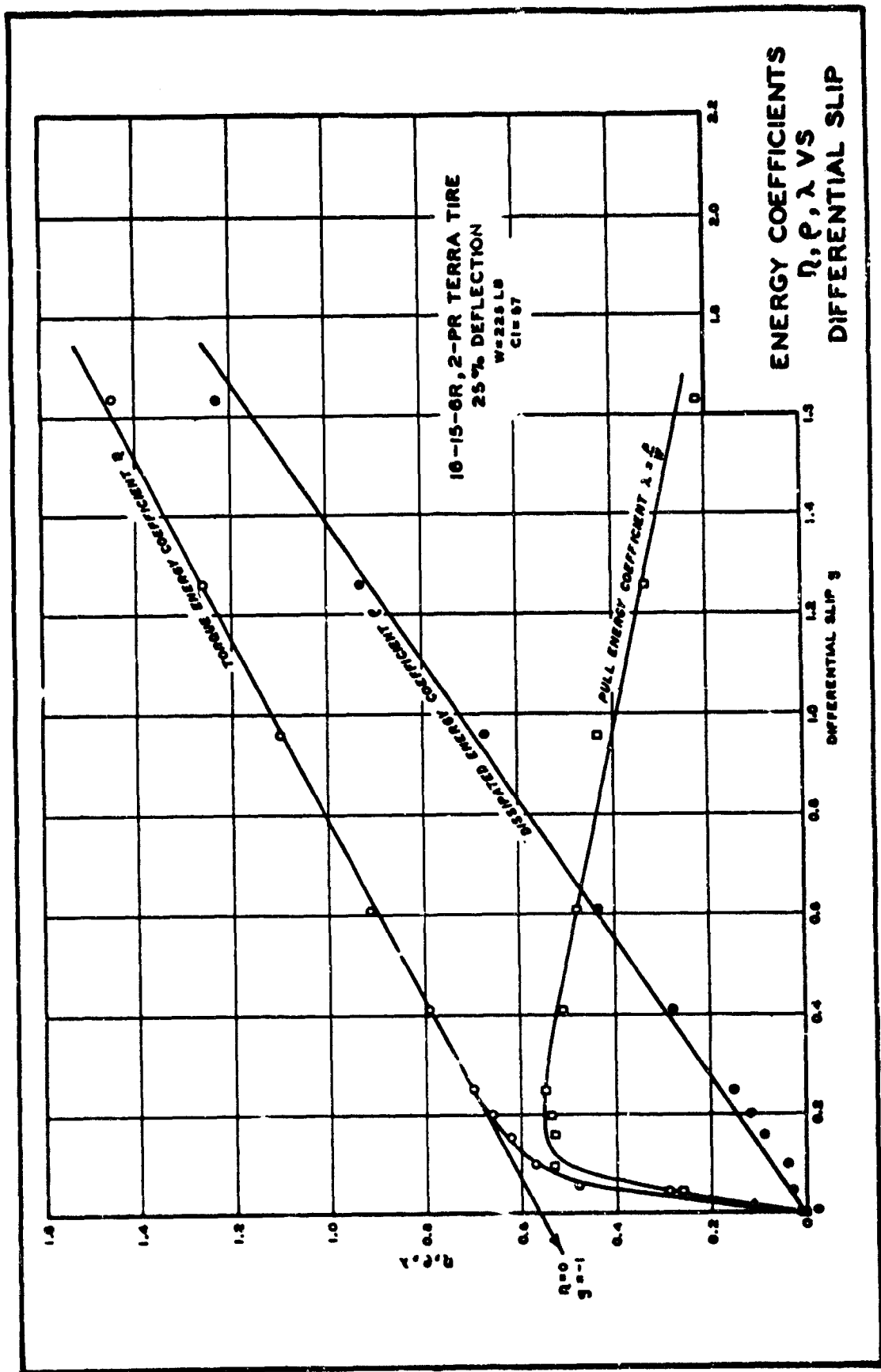


PLATE 3

# APPENDIX A: COMPARISON OF NORMAL SLIP AND DIFFERENTIAL SLIP

## Definitions

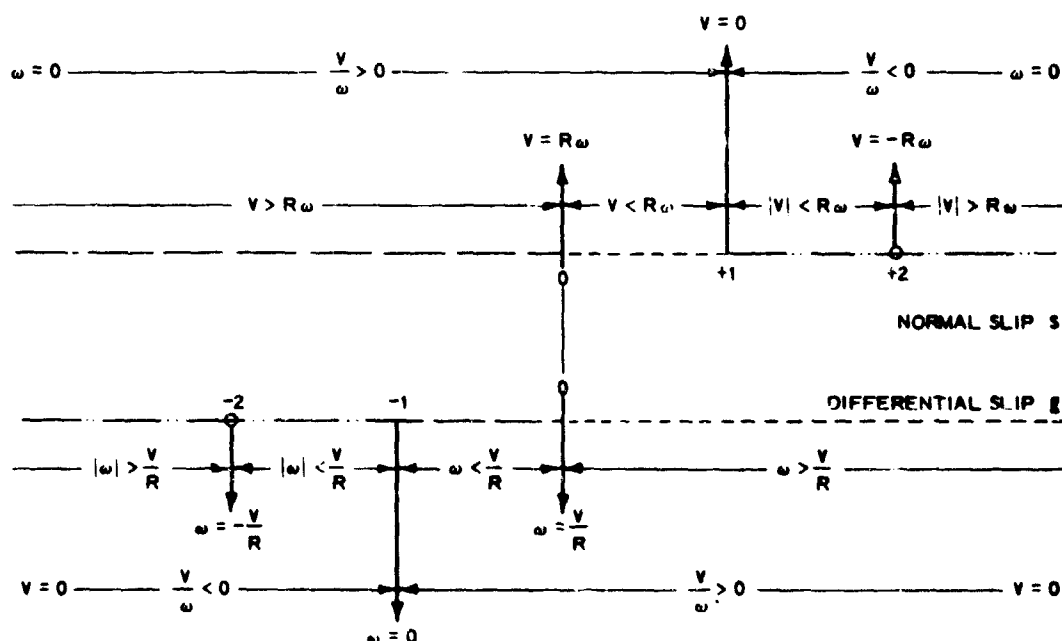
1. Normal slip  $s$  and differential slip  $g$  are defined as follows:

$$s = \frac{\text{theoretical velocity} - \text{actual velocity}}{\text{theoretical velocity}}$$

$$g = \frac{\text{theoretical velocity} - \text{actual velocity}}{\text{actual velocity}}$$

## Values of Normal and Differential Slip Under Various Operating Conditions of the Wheel

2. The operating conditions of the wheel that determine the magnitude of the slip are the relative values of forward speed  $v$ , rotational velocity  $\omega$ , and peripheral velocity  $R\omega$ . When  $v = R\omega$ , slip is zero; this is true for both normal and differential slip. In all other cases,  $s$  and  $g$  have different values. Fig. A1 summarizes the range of variations of  $s$  and  $g$  in all possible cases.



NOTE:  $v$  AND  $\omega$  ARE USED AS VARIABLES ON THE  $s$  AND  $g$  DIAGRAMS, RESPECTIVELY, TO AVOID CONSIDERING INFINITE VALUES OF  $v$  OR  $\omega$ .

Fig. A1. Correspondence of slip definitions

3. In fig. A1 the differing lines on the  $s$  and  $g$  axes indicate the range of variation of both slips in corresponding conditions. For instance, when normal slip  $s$  varies from 0 to 1, differential slip  $g$  varies from 0 to  $+\infty$ . Symmetrically, when  $s$  varies from 0 to  $-\infty$ ,  $g$  varies from 0 to -1. These ranges cover all conditions where rotation and movement of the wheel are in the same direction ( $\frac{v}{\omega} > 0$ ).

4. When the wheel is rotating opposite to its direction of movement ( $\frac{v}{\omega} < 0$ ), as in the case of a vehicle trying unsuccessfully to climb a slope and slipping back, the normal slip  $s$  varies from 1 to  $+\infty$ , and differential slip  $g$  varies from  $-\infty$  to -1. Thus, in this condition,  $s$  is positive and  $g$  is negative. It should be noted, however, that  $s$  and  $g$  always are increasing functions, each of the other. A unique condition occurs when  $v = -R\omega$ ; the wheel is rotating at the same velocity as it does for zero slip, but in the opposite direction. In this condition, normal slip  $s = +2$ , and differential slip  $g = -2$ .

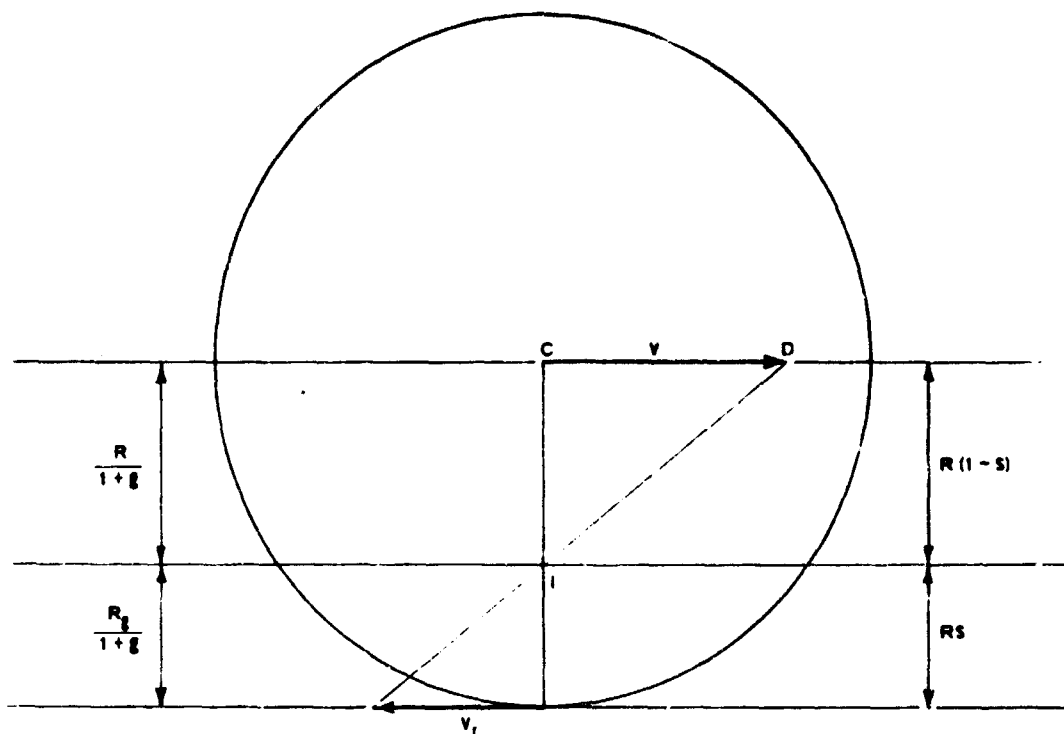
#### Properties of Normal and Differential Slip

5. Fig. A2 shows the relations among speed, normal slip, differential slip, position of the instantaneous center of rotation  $I$ , and rotational velocity of the wheel. In fig. A2 the angle  $\angle C I D$  is proportional to  $\omega$ ,  $v$  represents the forward velocity of the wheel axle, and  $v_r$  represents the velocity of a point on the wheel circumference as it passes the vertical plane through and below the axle center line. For a rigid wheel on a rigid surface,  $v_r$  is its relative speed at contact.

6. Fig. A2 illustrates the following:

##### a. For normal slip $s$ :

- (1) The distance traveled by the wheel in one revolution is  $2\pi \times CI = 2\pi R(1 - s)$ . Thus, the distance traveled per revolution is proportional to  $1 - s$ .
- (2) Normal slip is proportional to the distance between the instantaneous center of rotation and the lowest point of the wheel. Thus, the relative contact speed  $v_r$  is proportional to  $s$ .



$$V = R(1-g)\omega = \frac{R\omega}{1+g}$$

$$V_I = RS\omega = \frac{Rg\omega}{1+g}$$

Fig. A2. Geometrical representation of differential slip and normal slip

b. For differential slip  $g$ :

- (1) The number of revolutions per unit of distance traveled by the wheel is  $\frac{1}{2\pi \times CI} = \frac{1+g}{2\pi R}$ . Therefore, the number of revolutions per unit of distance traveled is proportional to  $1+g$ . Similarly, the distance traveled per revolution is proportional to  $\frac{1}{1+g}$ .
- (2) The relative displacement at the contact between the wheel and the surface, when the wheel travels one unit of distance, is given by the ratio  $\frac{V}{V_I}$ . This ratio is equal to  $g$ . Thus, the ground-wheel displacement at contact, per unit of distance traveled, for a rigid wheel on a rigid surface is proportional to differential slip  $g$ .

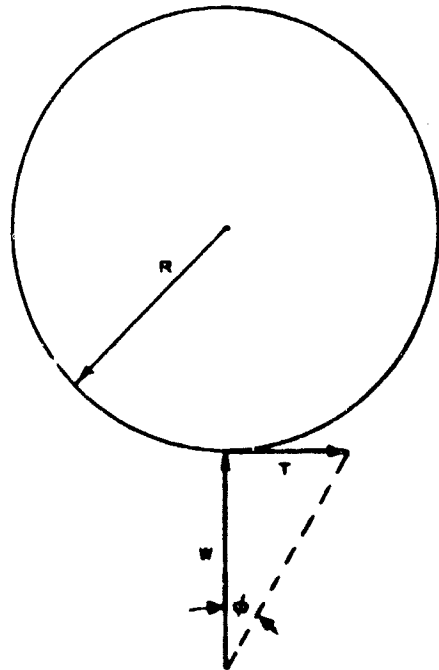
## APPENDIX B: INFLUENCE OF STRESS DISTRIBUTION ON TORQUE

1. The purpose of the study presented in this appendix is to determine how much the moment of the resultant of the stresses may vary along the circumference of a rigid wheel with respect to the wheel axle. Only the two-dimensional case is considered, and it is further assumed that:

- a. The tangential stress at every point of the wheel circumference is equal to the normal stress multiplied by a constant coefficient of friction  $\tan \phi$ . Consequently, the conclusions are valid only if the slip is large enough for this to be true.
- b. The resultant of the contact stresses has an inclination with respect to the vertical that varies with the test conditions, but its vertical component is always equal to the load  $W$  on the wheel. Thus, the value of the resultant is not constant when its inclination varies.

2. To provide a basis for analysis, the value of the torque  $M$  in the various cases is compared with the torque  $M_0$  occurring at the limiting condition represented in fig. B1, where the resultant is a concentrated

Fig. B1. Stress distribution on a wheel reduced to a unique force





force acting on the lowest point of the wheel (rigid wheel on rigid ground). This can be written

$$M_0 = WR \tan \phi \quad (B1)$$

3. The value of the moment of the resultant of the contact stresses on a wheel in soil is affected by three elements:

- a. The inclination of the resultant, which has a constant vertical component  $W$ .
- b. The extent of the arc on which stresses are acting; i.e. the extent of the distribution.
- c. The shape of the distribution.

4. In this study a symmetrical distribution is assumed; therefore, the inclination of the resultant can be represented by the angle  $\alpha$  (see fig. B2) formed by the bisecting line of the distribution and the vertical. Actually,  $\alpha$  represents the inclination of the distribution as well as

that of the resultant. The extent of the distribution is measured by  $\beta$ .

5. Two extreme cases of the shape of the stress distribution, assuming no tension between the soil and the wheel, can be hypothesized as (a) one concentrated force and (b) two concentrated forces at the extremities of the contact arc. Since the second condition is very unlikely in practice, a third case is considered, which is a uniform stress distribution along the arc of contact. It is reasonable to state, at least for sand, that the actual distribution is between the concentrated force and the uniform distribution. The effects of the

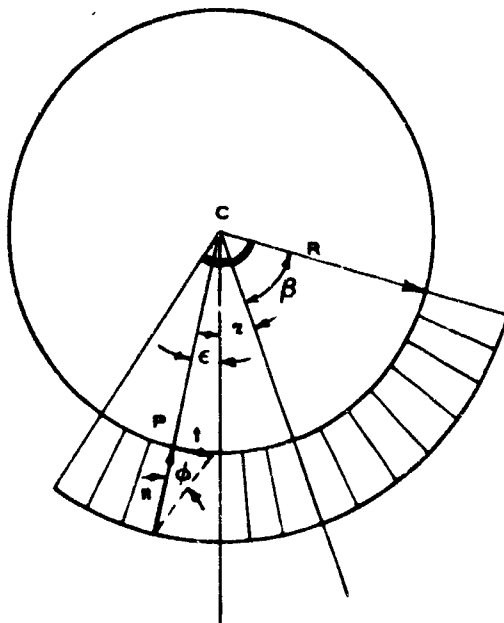


Fig. B2. Uniform stress distribution on a wheel, definition of angles

inclination of the resultant and of the extent of the stress distribution were evaluated by the study of the uniform distribution in fig. B2. This distribution can be characterized by the parameters  $\alpha$  and  $\beta$ , and the stress magnitude  $n$ . With angle  $\epsilon$  to an arbitrary point  $P$  on the arc of contact as the variable,

$$t = n \tan \phi$$

$$M = \int_{\alpha-\beta}^{\alpha+\beta} tR^2 d\epsilon = 2\beta tR^2 - \beta R (2tR) \quad (B2)$$

6. The angle  $\alpha$  does not appear in the equation because the condition that the vertical component of the resultant is  $W$  has not yet been stated. This is expressed by the equation:

$$W = \int_{\alpha-\beta}^{\alpha+\beta} (n \cos \epsilon + t \sin \epsilon) R d\epsilon$$

Then, since  $t = n \tan \phi$ , or  $n = t \frac{\cos \phi}{\sin \phi}$ ,

$$\begin{aligned} W &= \int_{\alpha-\beta}^{\alpha+\beta} \left( t \frac{\cos \phi}{\sin \phi} \cos \epsilon + t \sin \epsilon \right) R d\epsilon \\ &= \frac{tR}{\sin \phi} \int_{\alpha-\beta}^{\alpha+\beta} (\cos \phi \cos \epsilon + \sin \phi \sin \epsilon) d\epsilon \\ &= \frac{tR}{\sin \phi} \int_{\alpha-\beta}^{\alpha+\beta} \cos (\phi - \epsilon) d\epsilon \\ &= \frac{tR}{\sin \phi} \left[ \sin (\epsilon - \phi) \right]_{\alpha-\beta}^{\alpha+\beta} \\ &= \frac{tR}{\sin \phi} [\sin (\alpha + \beta - \phi) - \sin (\alpha - \beta - \phi)] \\ &= \frac{tR}{\sin \phi} [2 \sin \beta \cos (\alpha - \phi)] \end{aligned}$$

Consequently,

$$2tR = \frac{W \sin \phi}{\sin \beta \cos (\alpha - \phi)}$$

and then combining with equation B2,

$$M = \frac{\beta R W \sin \phi}{\sin \beta \cos (\phi - \alpha)} \quad (B3)$$

From equation B1,  $M_0 = WR \frac{\sin \phi}{\cos \phi}$ , or  $M_0 \cos \phi = WR \sin \phi$ .  
Then substituting this in equation B3,

$$M = M_0 \frac{\beta}{\sin \beta} \frac{\cos \phi}{\cos (\phi - \alpha)} \quad (B4)$$

7. The effect of the extent of the distribution is expressed by the factor  $\frac{\beta}{\sin \beta}$ . In the case of a concentrated force,  $\beta = 0$  and  $\frac{\beta}{\sin \beta} = 1$ . The maximum deviation of the torque for which the distribution is responsible is the difference between 1 and  $\frac{\beta}{\sin \beta}$  for each value of  $\beta$ . The actual deviation is a fraction of the deviation corresponding to a uniform distribution. The moment increases when  $\beta$  increases, according to the following tabulation (uniform distribution):

$\beta$ , deg	0	5	10	15	20	25	30	35	40	45
Increase of M due to factor $\frac{\beta}{\sin \beta}$ (percent)	0	0	1	1	2	3	5	6	8	10

8. The effect of the inclination of the resultant is expressed by the factor  $\frac{\cos \phi}{\cos (\phi - \alpha)}$ ; for a concentrated force,

$$M = M_0 \frac{\cos \phi}{\cos (\phi - \alpha)} \quad (B5)$$

This expression describes the influence of the inclination of the resultant with respect to the vertical when the vertical component  $W$  is constant. For  $\alpha$  between 0 and  $\phi$ ,  $M$  decreases when  $\alpha$  increases.  $M$  has a minimum value for  $\alpha = \phi$ , and then increases with increasing  $\alpha$  for

$\alpha > \phi$ . The amount of the deviation is given in the following tabulation  
for  $\phi = 30$  deg :

$\alpha$ , deg	0	5	10	15	20	25	30	35	40	45
Deviation of M due to factor $\frac{\cos \phi}{\cos (\phi - \alpha)}$ (percent)	0	-4	-8	-10	-12	-13	-13	-13	-12	-10

## APPENDIX C: ROTATIONAL DIRECT SHEAR TESTS ON YUMA SAND

1. The desirability of comparing the slopes of the  $\eta$  versus  $g$  curves and the angle of friction of the sand was discussed in paragraph 36 in the main text. Plate 1 in the main text shows straight lines for relatively large slip values. Since large slips imply large deformations, large-deformation shear tests were performed on Yuma sand to determine the ultimate angle of friction.

2. The tests were conducted with the Hvorslev rotational direct shear test apparatus.\* For practical reasons, most of the tests were made using divided rings for the annular shear box; thus, the shear box was made of two halves separated during the test by a narrow spacing. It was necessary to keep this spacing as small as possible during the shearing process to avoid sand flow through it, if a plane strain condition was to be realized. With such precautions, very consistent test results were obtained, giving a horizontal stress  $\tau$  over vertical stress  $\sigma_v$  ratio of 0.61, corresponding to an angle of friction  $\phi$  of  $31\text{-}1/2$  deg (see table C1).

3. Since a plane strain condition does not occur under a moving wheel, an investigation was made of the effect of the width of the spacing between the rings of the annular shear box on the apparent angle of friction. The results showed a regular decrease in the apparent shear strength from 0.61 for a spacing between 0 and 0.5 mm to 0.4 for a 3-mm spacing. This was due to the different limiting conditions for deformation in the shear zone. It is similar to the effect of the lateral movement of the sand under a wheel, which leads to an apparent angle of friction smaller than  $31\text{-}1/2$  deg, the slope of  $\eta$  versus  $g$  curves (see table C1 and fig. C1).

4. It is not possible to make a direct comparison between the deformation conditions in the rotational shear test and those under a wheel. However, test results show that the decrease in apparent shear strength in both conditions is of the same magnitude, which confirms the importance of this effect on the performance of a wheel. An approach using the concept

---

\* U. S. Army Engineer Waterways Experiment Station, CE. Torsion Shear Apparatus and Testing Procedures, Bulletin No. 38, Vicksburg Miss., May 52.

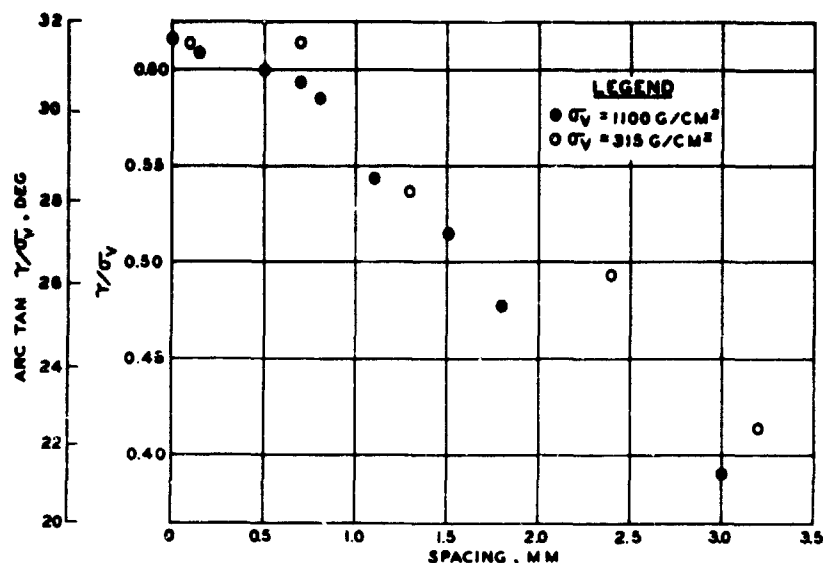


Fig. C1. Effect of spacing between the rings in rotational direct shear tests on Yuma sand

of the geometrical anisotropy of the sand may lead to a theoretical relation between the conditions of deformation and the stresses within a sand mass, and thus explain the influence of the conditions of deformation of the sand under a wheel. A complete analysis of the flow pattern, however, is much too complex to be considered in every detail.

Table C1  
Torsion Shear Test Results, Yuma Sand

Test No.	Vertical Stress $\sigma_v$ , kg/cm <sup>2</sup>	Spacing, mm	Shear Stress $\tau$ , g/cm <sup>2</sup>	$\tau/\sigma_v$
<u>Undivided Ring</u>				
10	0.6	--	372	0.630
		--	352	0.595
11	0.6	--	352	0.595
	1.1	--	641	0.582
<u>Divided Rings</u>				
3	0.6	0.5	372	0.605*
	1.1	0.5	685	0.614
4	0.6	0.5	372	0.605
5	0.6	0.5	376	0.610
	1.1	0.5	677	0.610
9	0.3	0.5	194	0.614
14	1.1	0.5	687	0.616
		0.5	676	0.609
<u>Effect of the Spacing Between the Rings</u>				
9	0.3	0.1	194	0.614
		0.7	194	0.614
		1.3	170	0.537
		2.4	156	0.493
		3.2	130	0.414
14	1.1	0.0	687	0.616
		0.15	676	0.609
		0.5	669	0.600
		0.7	662	0.594
		0.8	653	0.585
		1.1	605	0.543
		1.5	574	0.515
		1.8	535	0.478
		3.0	435	0.390

\* The average  $\tau/\sigma_v$  for the divided rings is 0.610;  $\arctan 0.61 = 31-1/2$  deg.

## APPENDIX D: CRITERIA FOR PROPELLING-SYSTEM EFFICIENCY

### Size and Efficiency

1. It is recognized that efficiency of a propelling system is important when considering costs. However, efficiency also is important with regard to the dimensions of the system, its fuel consumption, and the requirements of supply. Thus, it is a criterion worthy of consideration in the study of vehicle mobility. However, only efficiency of the soil-wheel system is considered in this study, without regard to efficiency of other vehicle components.

2. For propelling systems supported by deformable media, a dilemma exists between the size of the propelling system and the propulsion efficiency. The propulsive force is obtained by deformation of the medium and is an increasing function of that deformation and of the area of action of the propelling system on the medium. However, deformation also dissipates energy, and for all media, as deformation increases, energy dissipation increases faster than the increase in propulsive energy obtained. Therefore, an increase in deformation results in a decrease in efficiency.

3. Thus, if a given propulsive force is required, two parameters may be acted upon: the area of action of the system, and the amount of deformation of the medium. Deformation must be decreased to increase efficiency; therefore, to keep the propulsive force constant, the area of action of the propelling system must be increased. This can be done in either of two ways: by increasing the overall dimensions of the propelling system, or by modifying its configuration keeping size constant. For vehicles operating on soil, modification can be accomplished, for example, by reducing inflation pressure of the tires or by adopting a track configuration. If this does not produce the desired efficiency, dimensions must be increased as in the case of the very large wheel diameters (compared with vehicle size) of a farm tractor.

4. This reasoning is generally valid for propulsion through deformable media. It is also valid for boat or aircraft propellers, where the



necessity for a compromise between size and efficiency has long been recognized. The following example illustrates the dilemma between efficiency and size for an air propeller. It is assumed that propelling a car at 67 mph required a power of 20 kw. To furnish this power, a propeller 8 in. in diameter would require a power of 60 kw, obviously inefficient. A propeller 8 ft in diameter would require only 21 kw, but is out of proportion to the size of the vehicle.\* The problem of wheels on deformable soils presents an analogous situation, except that the mechanisms used to increase the size of the propelling system or to modify its configuration are peculiar to soil-wheel systems.

### Means of Expressing Efficiency

#### Review of efficiency coefficients

5. A review of coefficients of efficiency used or proposed by various authors or laboratories is given below. These coefficients were taken from existing literature on efficiency of wheels in soft soils. When not stated otherwise, definitions were taken from the proceedings of the First International Conference on the Mechanics of Soil-Vehicle Systems held in Turin, Italy, in 1961.

#### a. U. S. Army Engineer Waterways Experiment Station:

$$\text{Towed force coefficient} = \frac{P_T}{W}$$

$$\text{Drawbar pull coefficient} = \frac{P_M}{W}$$

$$\text{Traction coefficient} = \frac{P_M + P_T}{W}$$

where  $P_T$  = towed force  
 $P_M$  = maximum pull  
 $W$  = load

---

\* S. Boudigues, "Defense et illustration des propulseurs pour avions rapides (Defence and illustration of propelling systems for fast airplanes)."

In this definition, the pull and the towed force are referenced to the same sinkage.

b. Vehicle Mobility Laboratory, Canadian Army:\*

$$\text{Drawbar coefficient} = \frac{P}{W}$$

$$\text{Optimum drawbar coefficient, or mobility index} = \frac{P_{\text{opt}}}{W}$$

where  $P$  = pull

$P_{\text{opt}}$  is defined for a track by the maximum of the curve  $\frac{P \cdot v}{W \cdot v_t}$  versus slip  $s$ , where

$v$  = vehicle speed

$v_t$  = track speed

The equivalent for a wheel would be the maximum of  $\frac{P}{W} (1 - s)$  versus slip  $s$ . The optimum is the pull occurring at the slip of the maximum of the curve.

$$\text{Drawbar efficiency} = \frac{Pv}{\text{power input}} ; \text{ for a wheel, } \frac{Pv}{Mv}$$

$$\text{Load-carrying index} = \frac{Lv}{\text{power input}} ; \text{ for a wheel, } \frac{Lv}{Mv}$$

where  $L$  = payload

c. U. S. Department of Agriculture National Tillage Machinery Laboratory:\*\*

$$\text{Coefficient of traction} = \frac{P}{W}$$

$$\text{Power efficiency} = \frac{Pv}{Mv}$$

---

\* W. J. Dickson, "Ground vehicle mobility on soft terrain," Proceedings, American Society of Civil Engineers, No. SM4, vol 88, Paper 3225 (August 1962), pp 126-129.

\*\* G. E. Vandenberg and I. F. Reed, "Tractive performance of radial-ply and conventional tractor tires," Transactions, American Society of Agricultural Engineers, General edition, vol 5, No. 2 (1962), pp 126-129, 132.

Performance factor = coefficient of traction x power efficiency

$$\text{Coefficient of rolling resistance } \rho = \frac{M_D}{W_v} - \frac{P}{W}$$

$$\text{Travel efficiency} = 1 - s$$

d. Stevens Institute of Technology:\*\*

$$\text{Power efficiency} = \frac{P_v}{M_D}$$

e. F. L. Uffelmann (Fighting Vehicles Research and Development Establishment, Chertsey, England):

Tractive soil reaction = horizontal component of the resultant of the tangential stresses on the wheel

Rolling resistance = towed force

f. J. R. Phillips (University of Western Australia):

$$\text{Coefficient of rolling resistance } \rho = \frac{M_D}{W_v} - \frac{P}{W} = \frac{M_D - P_v}{W_v}$$

g. G. S. Steinbruegge (University of Nebraska):

$$\text{Soil tractive efficiency} = \frac{P}{I + \frac{\text{soil energy losses}}{\text{distance of travel}}}$$

This definition assumes that soil energy losses can be determined directly by theory.

Functions of vehicles

6. A single definition of efficiency of a soil-wheel system is difficult to justify because, at least mechanically, the wheel is used for two different purposes: (a) to act as a machine in which torque is transformed into pull as in a tractor, or (b) to propel itself without production of a pull as in a four-wheel-drive vehicle (at least on level ground, with air resistance ignored). Both uses are important, and one coefficient, regardless of how refined its definition, cannot adequately express both qualities of a system. For example, if efficiency is expressed in pull,

---

\* J. R. Phillips, op cit, p 1.

\*\* C. W. Wilson and J. P. Finelli, A Progress Report of Tests on Military Type Pneumatic Tires, Stevens Institute of Technology, Experimental Towing Tank Report No. 570, Hoboken, New Jersey, November 1955.

any self-propelled vehicle, no matter what its qualities, always has zero efficiency. Since the tractive function and the load-carrying function are often combined, a coefficient of efficiency will have to be an arbitrary compromise, depending on the relative importance of each function in a given case.

#### Total efficiency

7. The simplest coefficient to express the efficiency of a wheel acting as a machine to transform torque energy into traction energy is the expression  $\frac{P_v}{M_{\omega}}$ . This ratio is often called power efficiency, but since many other possible ratios are also power ratios, it is proposed to denote this ratio by the term "total efficiency" to show that it is the ratio of recoverable energy to total energy input.

8. Expressed in terms of the quantities used in this report,

$$\frac{P_v}{M_{\omega}} = \frac{P}{W} \cdot \frac{Wv}{M_{\omega}} = \frac{\lambda}{\eta}$$

This ratio is denoted  $\mu$ . For a rigid wheel on a hard surface,

$$\mu = \frac{\lambda}{\eta} = \frac{f}{f(1+g)} = \frac{1}{1+g} = 1 - s$$

Thus, in the reference condition, total efficiency  $\mu$  is identical with  $1 - s$ , a factor called travel reduction or travel efficiency by others. The formula  $\mu = 1 - s$  holds for positive slip. A definition of efficiency for negative slip (in the reference system for a braking condition) has not yet been considered necessary.

#### Traction efficiency

9. Total efficiency  $\mu$  considers the vehicle only as a machine producing a pull. To include the fact that it is moving at the same time, energy needed to move the vehicle with no pull must be considered separately from the energy employed to produce pull. The energy at zero pull is the energy input in the condition of self-propulsion and is denoted  $\eta_a$ . The difference  $\eta - \eta_a$  is the additional energy input needed to produce a pull. To express how well this energy is used, "traction efficiency" is defined as the ratio  $\tau = \frac{\lambda}{\eta - \eta_a}$ . (In the ideal case of the rigid wheel

on rigid ground,  $\eta_a$  is zero; then, in that special case,  $\tau$  and  $\mu$  are identical.)

#### Self-propulsion index

10. When a wheel is just barely propelling itself, its pull-producing efficiency is zero. It is desirable, however, to have a way to compare energies required by different wheels under different conditions, so the self-propulsion index has been defined as  $\log_{10} \left( \frac{1}{\eta_a} \right)$ . It is the decimal

logarithm of the inverse of the energy required per unit of load per unit of distance traveled. In other words, if this energy is  $10^{-1}$ , the index is 1; if it is  $10^{-2}$ , the index is 2. This apparently sophisticated definition was selected to yield numbers of convenient use in a range compatible with achievable accuracy. Using the reciprocal of  $\eta_a$  gives an index such that the greater the index, the more efficient is the wheel performance. The logarithm is used to reduce the scale and thus avoid the illusion of a high degree of accuracy. According to this definition, the test results show that the 9.00-14 wheel with a 1200-lb load on a 35 cone index sand has an index of 1. The 16-15-6R Terra-Tire also has an index of 1 on the same strength sand, but with a 350-lb load. An increase or a decrease of 0.3 in the self-propulsion index means that the energy required to propel the wheel has changed approximately in a 2:1 ratio. The 16-15-6R Terra-Tire with a 200-lb load on 65 cone index sand has a self-propulsion index of 2, which means that it requires only one-tenth the energy that it does when the index is 1.

11. For a given wheel, the self-propulsion index is a function of load and soil strength. The performance of two self-propelled wheels can be compared by means of diagrams of the relation of the self-propulsion index to wheel load and soil cone index.

12. By analogy with the self-propulsion index, other indexes can be derived for defining the ability of a vehicle to carry a payload, for a towed vehicle or for a combination of powered and towed conditions.

#### Combination of Efficiency Coefficients and Indexes

13. The efficiency coefficients and self-propulsion index that have

been defined are essentially different, and there is no logical way to combine them. If a vehicle, with or without load, must move from one place to another and at the same time produce a pull, the two functions must be considered separately and the optimum condition defined empirically according to the circumstances. For example, there is no broad scientific definition of the efficiency for a vehicle climbing a slope unless the horizontal transportation is disregarded, because physics does not define the relative practical usefulness of lifting a vehicle a certain vertical distance while moving it horizontally another distance.

# DISTRIBUTION LIST

Address	No. of Copies
Commanding General, U. S. Army Materiel Command ATTN: AMCRD-DM ATTN: AMCRD-RV-E Washington, D. C.	1 2
Commanding Officer, USACRREL ATTN: Library Hanover, N. H.	1
Commanding Officer, USA Engineer Research and Development Laboratories ATTN: Technical Document Center Fort Belvoir, Va.	2
Commanding Officer, USA Electronics Research and Development Activity, Ariz. ATTN: SELHU-M Fort Huachuca, Ariz.	1
Commanding Officer, USA Electronics Research and Development Laboratories ATTN: SELRA/ADT Fort Monmouth, N. J.	1
Chief of Research and Development ATTN: Chief, Combat Materiel Division Department of the Army Washington, D. C.	1
Chief of Research and Development ATTN: CRD/M, Department of the Army Washington, D. C.	1
Chief of Research and Development Headquarters, Department of the Army ATTN: Director of Army Technical Information Washington, D. C.	3 copies of Form 1473
Defense Intelligence Agency ATTN: DIAAP-1E2 Washington, D. C.	1

Unclassified

Security Classification

DOCUMENT CONTROL DATA - RAD		
(Security classification of title, body of abstract and indexing annotation must be entered when the overall report is classified)		
1. ORIGINATING ACTIVITY (Corporate author) U. S. Army Engineer Waterways Experiment Station Vicksburg, Mississippi		2a. REPORT SECURITY CLASSIFICATION Unclassified
		2b. GROUP
3. REPORT TITLE  MECHANICS OF WHEELS ON SOFT SOILS; A METHOD OF ANALYZING TEST RESULTS		
4. DESCRIPTIVE NOTES (Type of report and inclusive dates) Final report		
5. AUTHOR(S) (Last name, first name, initial)  E. M. Leflaive		
6. REPORT DATE June 1966	7a. TOTAL NO. OF PAGES 45	7b. NO. OF REFS 7
8a. CONTRACT OR GRANT NO.  a. PROJECT NO.  c. Task No. 1-V-O-14501-B-52A-01  d.	9a. ORIGINATOR'S REPORT NUMBER(S) Technical Report No. 3-729	
		9b. OTHER REPORT NO(S) (Assign other numbers that may be assigned this report)
10. AVAILABILITY/LIMITATION NOTICES This document is subject to special export controls and each transmittal to foreign governments or foreign nationals may be made only with prior approval of U. S. Army Engineer Waterways Experiment Station.		
11. SUPPLEMENTARY NOTES	12. SPONSORING MILITARY ACTIVITY U. S. Army Materiel Command Washington, D. C.	
13. ABSTRACT <p>This report presents a method of analyzing the results of tests with pneumatic tires in sand. The method is based on considering the work of the pull developed by the test wheel as the difference between energy input and energy dissipation. The parameters used to represent these energies are defined, and their meanings are described in some detail by referring to the theoretical case of a rigid wheel on a rigid surface. This theoretical case is also used as a reference system to evaluate the results of actual tests. Experimental data for a number of representative test conditions are presented and compared with the reference system. Concepts of efficiency are introduced and discussed. It is concluded that the proposed approach is promising for both conveniently expressing experimental results and understanding tire behavior in soft soils. However, more data will have to be analyzed to draw quantitative conclusions for practical use. Four appendixes are included in which certain aspects of the definitions of slip, stress distribution, lateral confinement of sand, and criteria for propelling-system efficiency are discussed.</p>		

DD FORM 1473  
1 JAN 64

Unclassified

Security Classification



Unclassified  
Security Classification

14. KEY WORDS	LINK A		LINK B		LINK C	
	ROLE	WT	ROLE	WT	ROLE	WT
Sand						
Tires						
Trafficability						
Vehicle wheels						

INSTRUCTIONS

1. **ORIGINATING ACTIVITY:** Enter the name and address of the contractor, subcontractor, grantee, Department of Defense activity or other organization (corporate author) issuing the report.

2a. **REPORT SECURITY CLASSIFICATION:** Enter the overall security classification of the report. Indicate whether "Restricted Data" is included. Marking is to be in accordance with appropriate security regulations.

2b. **GROUP:** Automatic downgrading is specified in DoD Directive 5200.10 and Armed Forces Industrial Manual. Enter the group number. Also, when applicable, show that optional markings have been used for Group 3 and Group 4 as authorized.

3. **REPORT TITLE:** Enter the complete report title in all capital letters. Titles in all cases should be unclassified. If a meaningful title cannot be selected without classification, show title classification in all capitals in parenthesis immediately following the title.

4. **DESCRIPTIVE NOTES:** If appropriate, enter the type of report, e.g., interim, progress, summary, annual, or final. Give the inclusive dates when a specific reporting period is covered.

5. **AUTHOR(S):** Enter the name(s) of author(s) as shown on or in the report. Enter last name, first name, middle initial. If military, show rank and branch of service. The name of the principal author is an absolute minimum requirement.

6. **REPORT DATE:** Enter the date of the report as day, month, year, or month, year. If more than one date appears on the report, use date of publication.

7a. **TOTAL NUMBER OF PAGES:** The total page count should follow normal pagination procedures, i.e., enter the number of pages containing information.

7b. **NUMBER OF REFERENCES:** Enter the total number of references cited in the report.

8a. **CONTRACT OR GRANT NUMBER:** If appropriate, enter the applicable number of the contract or grant under which the report was written.

8b, 8c, & 8d. **PROJECT NUMBER:** Enter the appropriate military department identification, such as project number, subproject number, system numbers, task number, etc.

9a. **ORIGINATOR'S REPORT NUMBER(S):** Enter the official report number by which the document will be identified and controlled by the originating activity. This number must be unique to this report.

9b. **OTHER REPORT NUMBER(S):** If the report has been assigned any other report numbers (either by the originator or by the sponsor), also enter this number(s).

10. **AVAILABILITY/LIMITATION NOTICES:** Enter any limitations on further dissemination of the report, other than those imposed by security classification, using standard statements such as:

- (1) "Qualified requesters may obtain copies of this report from DDC."
- (2) "Foreign announcement and dissemination of this report by DDC is not authorized."
- (3) "U. S. Government agencies may obtain copies of this report directly from DDC. Other qualified DDC users shall request through \_\_\_\_\_."
- (4) "U. S. military agencies may obtain copies of this report directly from DDC. Other qualified users shall request through \_\_\_\_\_."
- (5) "All distribution of this report is controlled. Qualified DDC users shall request through \_\_\_\_\_."

If the report has been furnished to the Office of Technical Services, Department of Commerce, for sale to the public, indicate this fact and enter the price, if known.

11. **SUPPLEMENTARY NOTES:** Use for additional explanatory notes.

12. **SPONSORING MILITARY ACTIVITY:** Enter the name of the departmental project office or laboratory sponsoring (paying for) the research and development. Include address.

13. **ABSTRACT:** Enter an abstract giving a brief and factual summary of the document indicative of the report, even though it may also appear elsewhere in the body of the technical report. If additional space is required, a continuation sheet shall be attached.

It is highly desirable that the abstract of classified reports be unclassified. Each paragraph of the abstract shall end with an indication of the military security classification of the information in the paragraph, represented as (TS), (S), (C), or (U).

There is no limitation on the length of the abstract. However, the suggested length is from 150 to 225 words.

14. **KEY WORDS:** Key words are technically meaningful terms or short phrases that characterize a report and may be used as index entries for cataloging the report. Key words must be selected so that no security classification is required. Identifiers, such as equipment model designation, trade name, military project code name, geographic location, may be used as key words but will be followed by an indication of technical context. The assignment of links, rules, and weights is optional.

Unclassified  
Security Classification

<u>Address</u>	<u>No. of Copies</u>
Senior Engineer Instructor Office of Military Instruction, United States Corps of Cadets West Point, N. Y.	1
President U. S. Army Armor Board Fort Knox, Ky.	1
President U. S. Army Artillery Board Fort Sill, Okla.	1
President U. S. Army Infantry Board Fort Benning, Ga.	1
Commanding General, U. S. Army Weapons Command ATTN: AMSWE-RDR Rock Island, Ill.	1
Commanding General, U. S. Army Tank-Automotive Command ATTN: SMOTA-RCL Warren, Mich.	1
Commander, U. S. Army Forces Southern Command ATTN: Engineer Fort Amador, Canal Zone	1
Commanding General, U. S. Continental Army Command Engineer Division, DCSLOG ATTN: ATLOG-E-MB Fort Monroe, Va.	2
Commanding General, U. S. Continental Army Command ATTN: ATUTR-AVN Fort Monroe, Va.	1
Commandant, Command and General Staff College ATTN: Archives Fort Leavenworth, Kans.	1

<u>Address</u>	<u>No. of Copies</u>
Commanding Officer, U. S. Army Rock Island Arsenal ATTN: SWERI-RDD-RA Rock Island, Ill.	1
Commander, U. S. Army Picatinny Arsenal ATTN: SMUPA-VC1, Mr. D. Sen Dover, N. J.	1
Commanding Officer, Yuma Proving Ground ATTN: STEYT-TGM Yuma, Ariz.	1
Technical Library, Branch No. 4 U. S. Army Limited War Laboratory Aberdeen Proving Ground, Md.	1
Automotive Engineering Laboratory ATTN: STEAP-DP-LU Aberdeen Proving Ground, Md.	1
Commanding General, USA Test and Evaluation Command ATTN: Director, USA Development and Proof Services (Automotive Division) Aberdeen Proving Ground, Md.	1
Commanding Officer ATTN: Tech Library, Bldg 313 Aberdeen Proving Ground, Md.	2
Commanding Officer, U. S. Army General Equipment Test Activity Fort Lee, Va.	1
Chief, Crops Division U. S. Army Biological Laboratories Fort Detrick, Md.	1
Commanding Officer, U. S. Army Combat Developments Command Transportation Agency ATTN: Mr. Earl S. Brown Fort Eustis, Va.	1

<u>Address</u>	<u>No. of Copies</u>
Asst. Chief of Staff for Force Development Hqs, Department of the Army, ATTN: FOR DS SSS Washington, D. C.	1
United States Army Attaché, American Embassy U. S. Navy 100, Box 36 Fleet Post Office New York, N. Y.	2
Office of Naval Research ATTN: Geography Branch Department of the Navy Washington, D. C.	1
Office of Naval Research, Navy Department ATTN: Mr. Irv. Schiff (Code 493) Washington, D. C.	1
Commanding Officer, PHIBCB Two U. S. Naval Amphibious Base Little Creek, Norfolk, Va.	1
Commanding Officer, PHIBCB One U. S. Naval Amphibious Base Coronado, San Diego, Calif.	1
Commanding Officer and Director Naval Civil Engineering Laboratory Port Hueneme, Calif.	1
Director, Naval Warfare Research Center Stanford Research Institute Menlo Park, Calif.	1
Chief, Bureau of Yards and Docks ATTN: Code 42, Department of the Navy Washington, D. C.	2
Commanding Officer, U. S. Naval Photographic Interpretation Center Washington, D. C.	1

<u>Address</u>	<u>No. of Copies</u>
Chief, Combat Service Support Division Marine Corps Landing Force Development Center Marine Corps Schools Quantico, Va.	1
Commander, 3800th AB Wing, AU ATTN: BDCE-ED Maxwell AFB, Ala.	1
Headquarters, USAF (AFRSTC) Astronautics Division DCS/Research and Development Washington, D. C.	1
Commander, U. S. Strike Command ATTN: J4-E McDill AFB, Fla.	1
Commander, Air Proving Ground Command ATTN: PGBPS-12 Eglin AFB, Fla.	1
Headquarters, Tactical Air Command ATTN: DEUSA Langley AFB, Va.	2
Headquarters, U. S. Air Force Director of Civil Engineering (AFOCE-KA) Washington, D. C.	2
Headquarters, USAF Base Structures Branch, Directorate of Civil Engineering ATTN: AFOCE-CC Washington, D. C.	1
Commander, Hqs, Military Air Transport Service ATTN: MAMCE/FS Scott AFB, Ill.	1
Commander SEG (SEHB) Wright-Patterson AFB, Ohio	1
Systems Engineering Group, Deputy for Systems Engineering Directorate of Technical Publications and Specifications (SEFRR) Wright-Patterson AFB, Ohio	1

<u>Address</u>	<u>No. of Copies</u>
Air Force Weapons Laboratory ATTN: Civil Engineering Branch Kirtland AFB, N. Mex.	1
Terrestrial Sciences Lab (CRJT) Air Force Cambridge Res Lab, L. G. Hanscom Field Bedford, Mass.	1
Library, Division of Public Documents U. S. Government Printing Office Washington, D. C.	1
Library of Congress Documents Expediting Project Washington, D. C.	3
Defense Documentation Center, ATTN: Mr. Myer Kahn Cameron Station Alexandria, Va.	20
National Tillage Machinery Laboratory U. S. Department of Agriculture Auburn, Ala.	1
Mr. A. C. Orvedal, Chief, World Soil Geography Unit Soil Conservation Service Hyattsville, Md.	1
Chief, Crops Protection Branch Crops Research Division, Agricultural Research Service Beltsville, Md.	1
Director, Pacific Southwest Forest and Range Experiment Station, ATTN: Henry W. Anderson Berkeley, Calif.	1
U. S. Geological Survey Chief, Source Material Unit, Branch of Military Geology Washington, D. C.	2
Coastal Studies Institute Louisiana State University Baton Rouge, La.	1

<u>Address</u>	<u>No. of Copies</u>
New York University, School of Engineering and Science Research Division, University Heights New York, N. Y.	1
Ohio University Engineering Experiment Station ATTN: Mr. Seth Bonder Columbus, Ohio	1
Professor L. C. Stuart University of Michigan Ann Arbor, Mich.	1
University of Arkansas, College of Engineering ATTN: Mr. Henry H. Hicks, Jr. Fayetteville, Ark.	1
Dr. Clark N. Crain, Director Project DUTY Department of Geography, University of Denver Denver, Colo.	1
Stanford Research Institute ATTN: Mr. Gordon S. Wiley Menlo Park, Calif.	1
Engineering Societies Library New York, N. Y.	1
Highway Research Board Washington, D. C.	1
Research Analysis Corporation ATTN: Library Bethesda, Md.	1
Davidson Laboratory, Stevens Institute of Technology ATTN: Dr. I. R. Ehrlich Hoboken, N. J.	1

<u>Address</u>	<u>No. of Copies</u>
Wilson, Nuttall, Raimond Engineers, Inc. ATTN: Library Chestertown, Md.	1
Battelle Memorial Institute, ATTN: RACIC Columbus, Ohio	1

Consultants

Dr. A. A. Warlam	1
Prof. Robert Horonjeff	1
Mr. C. J. Nuttall	1
Dr. R. E. Fadum	1
Dr. N. M. Newmark	1
Prof. Gerald Pickett	1
Prof. W. F. Buchele	1